Journal of Statistical Physics, Vol. 86, Nos. 5/6, 1997

Dynamics of the Schlögl Models on Lattices of Low Spatial Dimension

S. Prakash[1,2] **and G. Nicolis**[1]

Received October 2, 1995; final September 9, 1996

The steady states and dynamics of the two Schlögl models on one- and two-dimensional lattices are studied using master equation techniques in tandem with simulations. It is found that the classic bistable behavior of model II is modified to monostable behavior at low dimension. An explanation of this modification is proposed in terms of the effective potential that appears in the dynamical equations on considering the significant effect of fluctuation correlations. The behavior can be modeled by replacing the transient average fluctuation correlation by its asymptotic value plus Gaussian white noise and analyzing the resulting effective potential obtained from the Fokker–Planck equation with multiplicative noise. For model I the transcritical bifurcation point is shifted to lower values of the forward rate k_2 of the second step of the reaction scheme and this shift can also be explained via an effective potential as a function of the average asymptotic fluctuation correlation. Further addition of noise to the asymptotic value is irrelevant for this model since the noise term in the corresponding Fokker–Planck equation turns out to be purely additive.

KEY WORDS: Lattice models; master equations; low-dimensional systems; nonequilibrium phenomena; nonlinear dynamics; dissipative systems; chemical reactions.

1. INTRODUCTION

The study of the effect of fluctuations on the macroscopic behavior of low-dimensional systems has been a subject of intensive research for many years. The existence of substantial fluctuation correlations in these systems has been found to drastically change their behavior from that of the mean

[1] Center for Nonlinear Phenomena and Complex Systems, Université Libre de Bruxelles, 1050 Brussels, Belgium.

[2] Present address: Laboratoire de Physique des Solides, Université de Paris-Sud, 91405 Orsay, France.

0022-4715/97/0300-1289$12.50/0

field (MF) valid at high dimension. The crossover from dimension-dependent behavior at low dimensions to MF behavior at some "upper critical dimension" has been investigated for many different kinds of statistical systems, ranging from spin models[1] to random walks[2] and chemical reactions.[3,4] For chemical reactions this crossover has been found to occur at a critical average coordination number of the lattice that depends on the molecularity of the reaction or the degree of nonlinearity of the dynamics.[5,6]

On the other hand, the study of systems far from equilibrium[7] has generated great interest and led to the observation of a wide variety of phenomena, ranging from those analogous to equilibrium thermodynamic phase transitions, such as bistability,[3] to chaos. The Schlögl models I and II[8] are prototypes of such nonequilibrium systems with the macroscopic rate laws describing second-order and first-order phase transitions, respectively, in the average steady-state concentration of X particles. They are comprised of the two reaction steps

$$\begin{aligned} A + (n-1)\,X &\underset{k_1'}{\overset{k_1}{\rightleftharpoons}} nX \\ X &\underset{k_2'}{\overset{k_2}{\rightleftharpoons}} B \end{aligned} \tag{1}$$

where $n=2$ for model I and $n=3$ for model II. The concentrations A and B of A and B particles are kept constant by contact with a reservoir or appropriate feeding; thus the concentration X is the only variable quantity in the macroscopic dynamics. The system is thus open and maintained at far-from-equilibrium conditions by controlling the value of the ratio of concentrations A/B far from its equilibrium value of $k_1'k_2'/k_1k_2$. In particular, model II is found to undergo a bifurcation to a bistable regime at certain critical values of the reservoir concentrations A and B. Within this regime the evolution of the system toward its steady state is found to be described by a quartic macroscopic potential with the system evolving to the minimum that is within the basin of attraction of its initial state.

Our aim in this paper is to study the Schlögl models (1) on one- and two-dimensional lattices in order to incorporate the microscopic constraints involved and to investigate the effect of fluctuations on such dissipative systems. We shall determine how the macroscopic steady states and dynamics of the system are modified by the presence of fluctuations due to their being embedded in a lattice of low dimension.

In Sections 2–4 we analyze the behavior of model II [$n=3$ in Eq. (1)] in one and two dimensions. In Section 2 we describe the macroscopic (MF) dynamics of the model and compare this with the behavior in low spatial

dimension as shown by results of simulations. In Section 3 we describe a model that is a variant of the full Schlögl model (1) and observe that it displays the same behavior as the full model in $d=1$ and $d=2$. We then proceed to solve for the dynamics of this model using a Glauber-type master equation formalism. The solution of the coupled differential equations thus obtained for the average concentration and the nearest neighbor (nn) fluctuation correlation are found to be almost identical to results of low-dimensional simulations. Making use of the functional form of these equations, we are able to explain the anomalous behavior of the model in low dimensions in terms of an effective potential that is quite different from the macroscopic one in the presence of significant fluctuation correlations. In Section 4 we present a more complete analysis of the effect of fluctuation correlations on the potential. Here the fluctuation correlations are treated as strong multiplicative noise and the corresponding Fokker–Planck equation yields the effective potential. We find that the fluctuation correlations turn the bistable macroscopic potential into an effectively monostable one with stable state at a concentration equal to or less than that of the lower stable state of the corresponding macroscopic potential.

In Section 5 we discuss the first Schlögl model [$n=2$ in (1)] and apply the methods of sections 2–4 to describe and explain its behavior on low-dimensional lattices. The transcritical bifurcation observed for the macroscopic case is found to be modified at low dimension. A sharp transition at a significantly lower value of k_2 is observed and can also be explained in terms of the effect of fluctuation correlations and the resulting effective potential.

All $d=1$ simulations reported in this paper were done on a ring of 10^4 particles averaged over 100 realizations. We also simulated systems of 10^5 particles and found no significant change in either the steady-state properties or the dynamics. We therefore retained the $N=10^4$ results for reasons of computational convenience. Similarly, all $d=2$ simulations were done on a 200×200 square lattice with periodic boundary conditions (i.e., a torus). Again, we also simulated 500×500 lattices to ensure by comparison the absence of finite-size effects in the smaller system.

2. SCHLÖGL II: MACROSCOPIC DYNAMICS AND SIMULATIONS

The macroscopic dynamics of Schlögl's second model [Eq. (1) with $n=3$] is described by the rate law

$$\frac{dX}{dt} = -k_1' X^3 + \alpha X^2 - k_2 X + \gamma = -\frac{\partial V_0(X)}{\partial X} \tag{2}$$

where we have set $\alpha = k_1 A$ and $\gamma = k_2' B$. Here $V_0(X)$ is the quartic macroscopic potential whose minima determine the stable states of the system. For $k_2' = 0$ and $k_2 \neq 0$ the system is bistable for $k_1' k_2 < \alpha^2/4$. There is a stable steady state at $X_1 = 0$ and the two other steady states are at $X_{3,2} = (\alpha \pm \sqrt{\alpha^2 - 4k_1' k_2})/2k_1'$; of these, X_2 is unstable and X_3 stable (see picture of potential on the right of Fig. 1). For $k_2' \neq 0$ and other parameters at values within the bistable regime the lower stable state is at $X_1 > 0$ (see right of Fig. 2). We shall frequently refer to the two sets of parameters used in Figs. 1 and 2, respectively, as parameter set 1 ($k_1 = 20.0$, $k_1' = 3.0$, $k_2 = 0.01$, $k_2' = 0.0$, $A = 0.1$, and $B = 0.05$) and parameter set 2 ($k_1 = 20.0$, $k_1' = 3.0$, $k_2 = 0.35133$, $k_2' = 0.36$, $A = 0.1$, and $B = 0.05$).

We simulate the dynamics of this model on one- and two-dimensional (square) lattices as follows: the first (trimolecular) step of Eq. (1) is realized as in ref. 9 with an A particle converting to X and vice versa with respective rates k_1 and k_1' if at least two of its neighbors is an X particle. The second (unimolecular) step is lattice independent, since the neighbors play no role. The concentrations of A and B particles are kept constant by randomly picking an A/B (vacant) site and removing (creating) an A/B every time one is created (removed) elsewhere by the Schlögl reaction. The results of these simulations are shown in Figs. 1 and 2 along with those of the corresponding macroscopic dynamics described by Eq. (2). We observe a striking difference between the behavior of the low-dimensional system and the

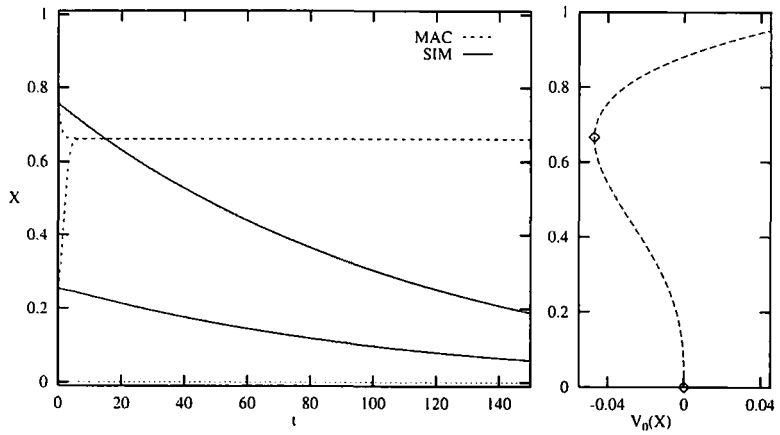

Fig. 1. Results of $d = 1 (z = 2)$ simulations (SIM) and solution of macroscopic equations (MAC) for the evolution of the concentration $X(t)$ for the second Schlögl model with parameter set 1 ($k_1 = 20.0$, $k_1' = 3.0$, $k_2 = 0.01$, and $k_2' = 0.0$). The concentrations of A and B particles are maintained at $A = 0.1$ and $B = 0.05$, respectively. The macroscopic potential V_0 with minima at $X_1 = 0$ and $X_3 = 0.66$ is shown at the right with diamonds marking the stable states.

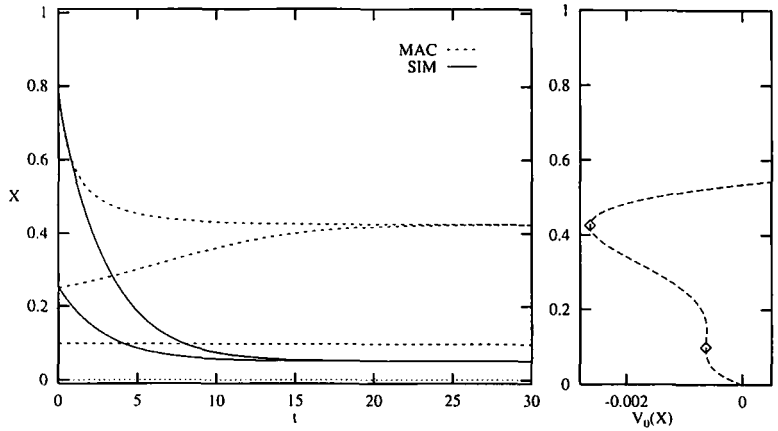

Fig. 2. Results of $d=1(z=2)$ simulations (SIM) and solution of macroscopic equations (MAC) for the evolution of the concentration $X(t)$ for the second Schlögl model with parameter set 2 ($k_1=20.0$, $k_1'=3.0$, $k_2=0.35133$, and $k_2'=0.36$). The concentrations of A and B particles are maintained at $A=0.1$ and $B=0.05$, respectively. The macroscopic potential V_0 with minima at $X_1=0.10$ and $X_3=0.42$ is shown at the right with diamonds marking the stable states.

corresponding macroscopic dynamics. For parameter set 1 with $k_2'=0$, where $X=0$ is stable, the one-dimensional system (coordination number $z=2$) always evolves to $X_1=0$ (see Fig. 1) even when the other steady state at X_3 is far more stable and the system is started above X_3 (see picture of potential on the right of Fig. 1). For parameter set 2 with $k_2'\neq 0$ the system evolves to a concentration that is clearly lower than that of the lower macroscopic steady state $X_1\neq 0$ (see Fig. 2), again even for the case when X_3 is more stable (potential on right). We note that the non-MF steady states realized by the low-dimensional system in this case are free of memory effects, unlike those observed in refs. 9 and 10 on low-dimensional lattices. Here the dependence on the initial states is only in the sense of bistability (i.e., which basin of attraction the initial state belongs to) and the steady-state concentration does not depend continuously on that of the initial state as in ref. 9.

In the following sections we explain this deviation from the macroscopic evolution equations in terms of the fluctuation correlations that modify the effective potential and thus the stable states and dynamics of the system.

3. TWO-SPECIES SCHLÖGL MODEL II

In order to develop analytic insight into the phenomena described above, we now consider a variation on the classic Schlögl model II. This

new model consists only of X and A particles that undergo the reaction steps

$$\begin{aligned} A + 2X &\underset{k_1'}{\overset{k_1}{\rightleftharpoons}} 3X \\ X &\underset{k_2'}{\overset{k_2}{\rightleftharpoons}} A \end{aligned} \tag{3}$$

The system is kept artificially far from equilibrium by maintaining $k_1'k_2'/k_1k_2 \neq 1$ without any reference to concentrations being kept constant by contact with reservoirs. In the context of chemical kinetics this may be achieved, for instance, by coupling one of the steps to an external field or to a catalytic cycle fed by a mechanism independent of the system at hand.

The lattice is kept fully occupied; thus $A = 1 - X$ and once again the concentration X can be taken to be the only variable in the macroscopic dynamics. We note that this model is also bistable and follows the macroscopic evolution equation

$$\frac{dX}{dt} = -(k_1 + k_1')X^3 + k_1X^2 - (k_2 + k_2')X + k_2' = -\frac{\partial V_0(X)}{\partial X} \tag{4}$$

Thus the macroscopic dynamics of this model is exactly the same as for the full Schlögl model (1) with the appropriate adjustment of parameters $\alpha \to k_1$, $k_1' \to k_1 + k_1'$, $k_2 \to k_2 + k_2'$; and $\gamma \to k_2'$.

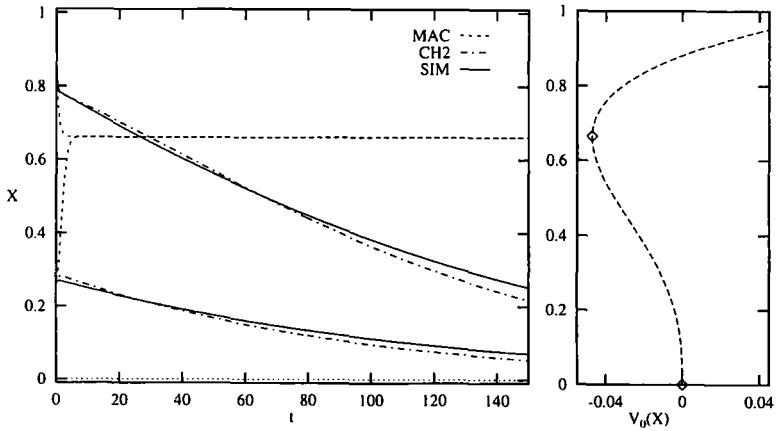

Fig. 3. Results of $d = 1$ ($z = 2$) simulations (SIM), solution of coupled differential equations (CH2), and solution of the macroscopic equations (MAC) for the evolution of the concentration $X(t)$ for the two-species trimolecular model with parameter set 1′ ($k_1 = 2.0$, $k_1' = 1.0$, $k_2 = 0.01$ and $k_2' = 0.0$). The macroscopic potential V_0 with minima at $X_1 = 0$ and $X_3 = 0.66$ is shown at the right with diamonds marking the stable states.

Next we simulate this model in one and two dimensions for two different sets of parameters equivalent to parameter sets 1 and 2 for the full Schlögl model to see how this model might deviate from the macroscopic behavior. These are parameter set 1′ ($k_1 = 2.0$, $k_1' = 1.0$, $k_2 = 0.01$, and $k_2' = 0.0$) and parameter set 2′ ($k_1 = 2.0$, $k_1' = 1.0$, $k_2 = 0.333$, and $k_2' = 0.018$). The results (see curves marked SIM in Figs. 3 and 4) indicate that this model behaves at low dimensions in an identical way to the full Schlögl model, evolving for $k_2 = 0$ to the lower stable state $X_1 = 0$ of the macroscopic potential $V_0(X)$ and for $k_2 \neq 0$ to a state *below* X_1. Thus, the additional compensatory dynamics of random creation and removal of A and B particles (to maintain their concentrations constant) in the full Schlögl model does not create any special features at this level. The combined role of vacancies and A and B particles in the full model is equivalent to that of A particles in the two-species model. In both models only two "species" change their relative concentration: for the full model it is X particles and vacancies and for the two-species model it is X and A particles. We also simulated this model on a square lattice ($d = 2$, $z = 4$) and found that the system with parameters 1′ now crosses over to the macroscopic steady state, while that with parameters 2′ behaves more or less like the corresponding one-dimensional system (see curves marked SIM Figs. 5 and 6).

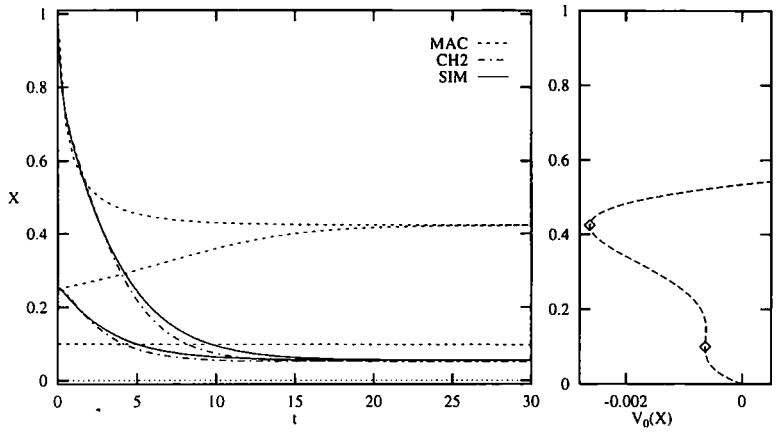

Fig. 4. Results of $d = 1$ ($z = 2$) simulations (SIM), solution of coupled differential equations (CH2), and solution of the macroscopic equations (MAC) for the evolution of the concentration $X(t)$ for the two-species trimolecular model with parameter set 2′ ($k_1 = 2.0$, $k_1' = 1.0$, $k_2 = 0.333$, and $k_2' = 0.018$). The macroscopic potential V_0 with minima at $X_1 = 0.10$ and $X_3 = 0.42$ is shown at the right with diamonds marking the stable states.

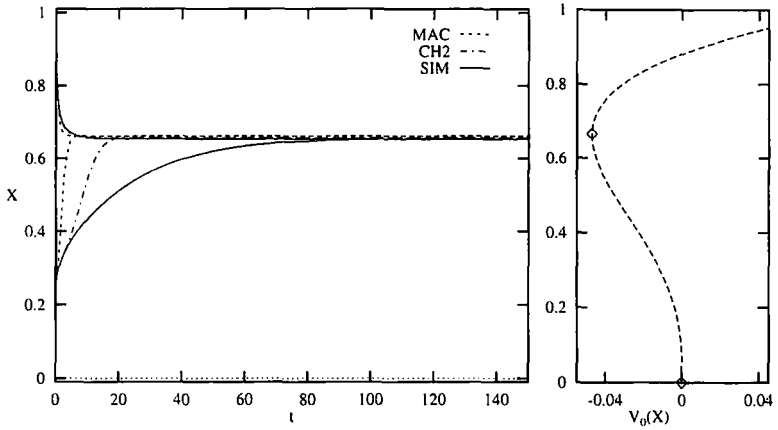

Fig. 5. Same as Fig. 3, for $d=2$ ($z=4$).

We shall now attempt to solve for the dynamics of this two-species model using a Glauber-type[11] master equation formulation similar to the one we used in ref. 9. We associate the X and A particles arranged on the sites i of a lattice of coordination number z with a set of N Ising spin-like variables $\sigma_i = \pm 1$. We adopt the convention $\sigma_i = +1$ (-1) if an A (X) particle is present at site i. We denote by $\{\sigma\}$ the configuration of Ising-like particles $(\sigma_1,..., \sigma_j,..., \sigma_N)$ and by $\{\sigma'\}$ the configuration $(\sigma_1,..., -\sigma_j,..., \sigma_N)$ obtained by changing the state of the particle at site j. Starting from some arbitrary initial state, the evolution of the probability distribution

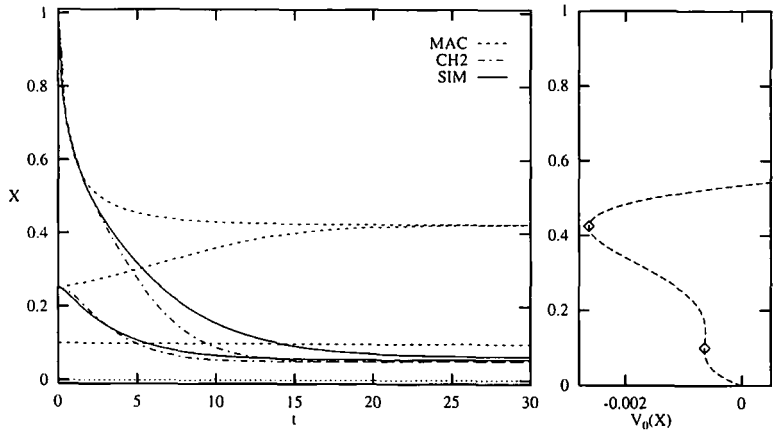

Fig. 6. Same as Fig. 4, $d=2$ ($z=4$).

$P(\{\sigma\};t)$ of the set of variables $\{\sigma\}=(\sigma_1,...,\sigma_j,...,\sigma_N)$ with time is described by the master equation[11]

$$\frac{dP(\{\sigma\};t)}{dt}=-\sum_j w_j(\{\sigma\}\to\{\sigma'\},t)\,P(\{\sigma\};t)+\sum_j w_j(\{\sigma'\}\to\{\sigma\},t)\,P(\{\sigma'\};t) \tag{5}$$

where we denote by $\{\sigma'\}$ the state $(\sigma_1,..., -\sigma_j,..., \sigma_N)$ and $w_j(\{\sigma\}\to\{\sigma'\},t)$ represents the transition probability per unit time from the state $\{\sigma\}$ to the state $\{\sigma'\}$ at time t.

The equation for the evolution of the average "magnetization" $q_k(t)=\langle\sigma_k(t)\rangle$ is then given by[11,9]

$$\frac{dq_k(t)}{dt}=-2\langle\sigma_k(t)\,w_k(\{\sigma\}\to\{\sigma'\},t)\rangle \tag{6}$$

and similarly the time evolution of the pair correlation function $r_{jk}(t)=\langle\sigma_j(t)\,\sigma_k(t)\rangle$ is described by (for $j\neq k$)

$$\frac{dr_{jk}(t)}{dt}=-2\langle\sigma_j(t)\,\sigma_k(t)[w_j(\{\sigma\}\to\{\sigma'\},t)+w_k(\{\sigma\}\to\{\sigma'\},t)]\rangle \tag{7}$$

with $j=k$ corresponding to the trivial case $r_{jj}(t)=1$ for all t.

Next we make the assumption of isotropy and translational invariance: thus

$$q_k(t)\to q(t)=A(t)-X(t) \tag{8}$$

is the concentration difference between the two species. Moreover, this implies that the pair correlation

$$r_{jk}(t)=\langle\sigma_j(t)\,\sigma_k(t)\rangle=q^2+f_n(t) \tag{9}$$

depends only on the distance $n=|k-j|$ between the sites with the fluctuation correlation $f_n(t)$ being given by

$$f_n(t)=\langle\delta\sigma_j(t)\,\delta\sigma_k(t)\rangle \tag{10}$$

So far the above formalism is completely general, i.e., we have made no assumptions about the nature of the local dynamics of the system as expressed in the form of the transition probabilities w_j. Now we apply this formalism to our two-species Schlögl model of Eq. (3) by

assigning the appropriate form to the transition probabilities. We write the contribution to the evolution of the average concentration difference $q(t)$ in two separate parts for the two steps (3) of the reaction:

$$\left(\frac{dq}{dt}\right)=\left(\frac{dq}{dt}\right)_1+\left(\frac{dq}{dt}\right)_2 \tag{11}$$

The flipping or transition probability w_j at site j for the first reaction on a lattice of coordination number z can be written as

$$w_j(\sigma_j \to -\sigma_j)=\left[\frac{k_1+k_1'}{2}+\frac{k_1-k_1'}{2}\sigma_j\right] w_j^0(\sigma_j \to -\sigma_j) \tag{12}$$

where w_j^0 is the transition probability for $k_1=k_1'=1$ and is given by

$$w_j^0(\sigma_j \to -\sigma_j)=\frac{2}{z(z-1)}\sum_{c_j, c_j'}\frac{1-\sigma_{c_j}}{2}\frac{1-\sigma_{c_j'}}{2} \tag{13}$$

with c_j and c_j' being two distinct nearest neighbors of the site j, i.e., $c_j \neq c_j'$.

This transition probability (12) is constructed to satisfy the conditions that it should be proportional to the probability of finding at least two X particles among the z neighbors $\{c_j\}$ of the particle at j and should also be proportional to k_1 if the site j contains an A particle and to k_1' if it contains an X particle.

Substituting Eq. (12) into Eq. (6) under the assumption (8) gives

$$\left(\frac{dq}{dt}\right)_1=-\frac{1}{4}(k_1-k_1')+\frac{1}{4}(k_1-3k_1')\,q+\frac{1}{4}(k_1+3k_1')\,q^2-\frac{1}{4}(k_1+k_1')\,q^3$$

$$+\frac{1}{2}(k_1+k_1')(f_1+f_2)-\frac{1}{2}(k_1+k_1')\,q(f_1+f_2)+O(\delta\sigma^3) \tag{14}$$

with f_1 and f_2 being the nearest neighbor and second neighbor correlations, respectively, defined in Eq. (10).

On the other hand, the second (unimolecular) reaction $X \rightleftharpoons A$ is a purely mean-field (MF) or macroscopic process in which the lattice and consequently the spatial fluctuations play no role. Thus the contribution of this process to (11) is given by

$$\left(\frac{dq}{dt}\right)_2=(k_2+k_2')\,q+(k_2-k_2') \tag{15}$$

For simplicity, we shall truncate the hierarchy of moments beyond $O(\delta\sigma^3)$ and also neglect all pair fluctuation correlations f_n for $n \geqslant 2$ (thus assuming strong short-range correlations between particles). We shall deal only with the pair of coupled equations for $q(t)$ and $f_1(t)$ (seed ref. 9 for details on the efficacy of this truncation procedure). Putting together Eqs. (14) and (15) and truncating beyond f_1, we get

$$\frac{dq}{dt} = -\frac{1}{4}(k_1 - k_1' - 4k_2 - 4k_2') + \frac{1}{4}(k_1 - 3k_1' - 4k_2 - 4k_2')\, q + \frac{1}{4}(k_1 + 3k_1')\, q^2$$

$$-\frac{1}{4}(k_1 + k_1')\, q^3 + \frac{1}{2}(k_1 + k_1')(1 - q)\, f_1 \tag{16}$$

In the MF limit $f_1 \to 0$ this reduces to the macroscopic evolution equation (4).

The evolution of the nearest neighbor fluctuation correlation $f_1(t)$ contains no contribution from the second step, since this is a purely MF process. Thus we have [from Eqs. (7), (12), and (13)] the evolution equation for $f_1(t) = r_{j,j+1}(t) - q^2(t)$:

$$\frac{df_1}{dt} = \frac{1}{z}(k_1 - k_1') + \frac{2k_1'}{z}\, q - \frac{2k_1}{z}\, q^2 - \frac{2k_1'}{z}\, q^3$$

$$+\frac{1}{z}(k_1 + k_1')\, q^4 - \frac{z+2}{2z}(k_1 + k_1')\, f_1$$

$$+\frac{z-2}{z}(k_1 + k_1')\, q f_1 + \frac{6-z}{2z}(k_1 + k_1')\, q^2 f_1 \tag{17}$$

Following the nomenclature used in ref. 9, we shall refer henceforth to the solution of this pair of coupled equations (16) and (17) as CH2. This solution for the concentration $X(t) = \frac{1}{2}[1 - q(t)]$ is shown for $d = 1 (z = 2)$ in Figs. 3 and 4 and for $d = 2 (z = 4)$ in Figs. 5 and 6 along with the results of simulations for two different initial states. We observe a very good agreement between theory (CH2) and simulation, especially in terms of the steady state value of the concentration $X(t \to \infty)$.

This behavior, in particular the deviation from the macroscopic steady state for these systems, can be described in terms of an altered effective potential resulting from the nonnegligible value of the fluctuation correlations $f_n(t)$ at low dimension. The evolution equation for $X(t)$ can be written in the simplified form [from Eq. (16)]

$$\frac{dX}{dt} = -\frac{\partial V_0(X)}{\partial X} - \frac{1}{2}(k_1 + k_1')\, X f_1 \tag{18}$$

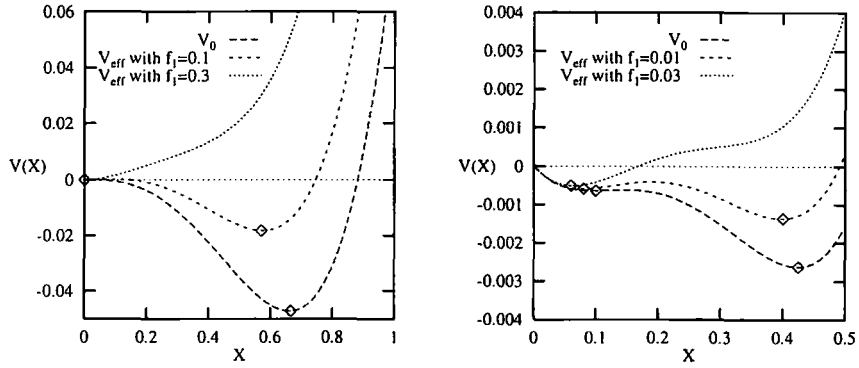

Fig. 7. Macroscopic potential $V_0(X)$ and effective potential $V_{\text{eff}}(X)$ for parameter sets 1′ (left) and 2′ (right). Minima are indicated by diamonds.

In the simplest approximation where the fluctuation correlation $f_1(t)$ is assigned a fixed value, we can describe the dynamics of the system via the effective potential $V_{\text{eff}}(X) = V_0(X) + V_{\text{fl}}(X)$, where the contribution from fluctuations is $V_{\text{fl}}(X) = \frac{1}{4}(k_1 + k_1')\, X^2 f_1$. A quick look at Fig. 7 is enough to see that the effective potential indeed describes qualitatively the anomalous dynamics of the low-dimensional system. For parameter set 1′ (left graph), the fluctuation term leads to a crossover from a bistable potential to one with a unique stable state at $X_1 = 0$. For parameter set 2′ (right graph), again one sees a crossover in the form of the potential, this time to one with a unique stable state clearly below the macroscopic lower stable state at $X_1 = 0.1$.

4. FLUCTUATION CORRELATIONS AS MULTIPLICATIVE NOISE

We now take a brief look at the form of the nn fluctuation correlation $f_1(t)$ as determined from simulations and from the solution (CH2) of the coupled pair of Eqs. (16) and (17). A comparison of Fig. 8 for the full Schlögl model and Fig. 9 for the two-species model for equivalent parameters (the same macroscopic potential) indicates the same qualitative behavior of the fluctuation correlations, though a difference in magnitude. However, the average (asymptotic) values of f_1 for the two-species model are considerably lower than those at which a transition to a monostable potential takes place. For example, for parameter set 1′ in the left graph of Fig. 9 the asymptotic value is $f_1(t \to \infty) = 0$; however, it requires a value $f_1 \simeq 0.3$ (see left graph of Fig. 7) for the transition to take place. Again, for parameter set 2′ in the right graph of Fig. 9 we have $f_1(t \to \infty) \simeq 0.01$ from

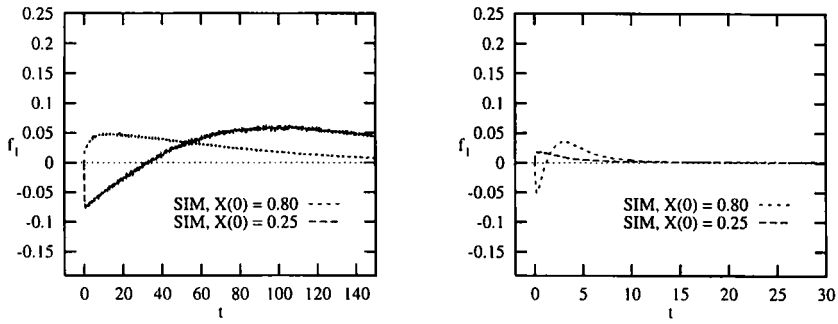

Fig. 8. Evolution of fluctuation correlation $f_1(t)$ for full Schlögl model II in $d=1(z=2)$ from simulations for parameter set 1 (left) and set 2 (right).

simulations, but once again it requires $f_1 \simeq 0.03$ (see right graph of Fig. 7) for a transition to a monostable potential.

We attribute this discrepancy to the significant short-time transient magnitude of the fluctuation correlation in Fig. 9. We shall now proceed to treat this transient as a perturbation about the asymptotic value $f_1(\infty)$. Thus we write

$$f_1(t) = f_1(\infty) + \xi_1(t) \tag{19}$$

where we shall assume the $\xi(t)$ to be Gaussian white noise, i.e.,

$$\langle \xi_i(t)\, \xi_j(t') \rangle = \varepsilon_i\, \delta(t-t')\, \delta_{ij} \tag{20}$$

with $\varepsilon_1 = \sigma^2$, σ being the width of the Gaussian distribution from which $\xi_1(t)$ is taken randomly. The width σ is to be compared with the width of

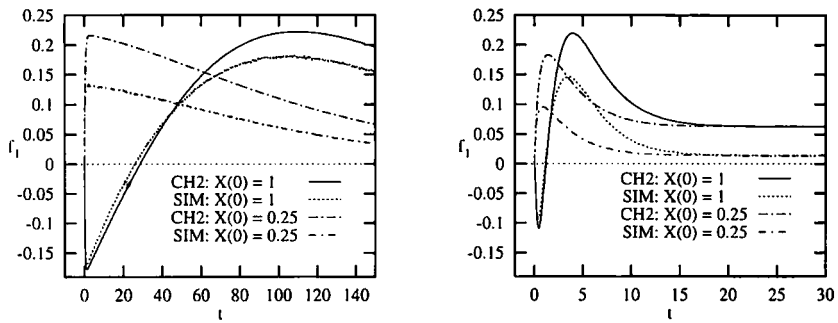

Fig. 9. Evolution of fluctuation correlation $f_1(t)$ for two-species trimolecular model in $d=1(z=2)$ from simulations (SIM) and CH2 for parameter sets 1′ (left) and 2′ (right).

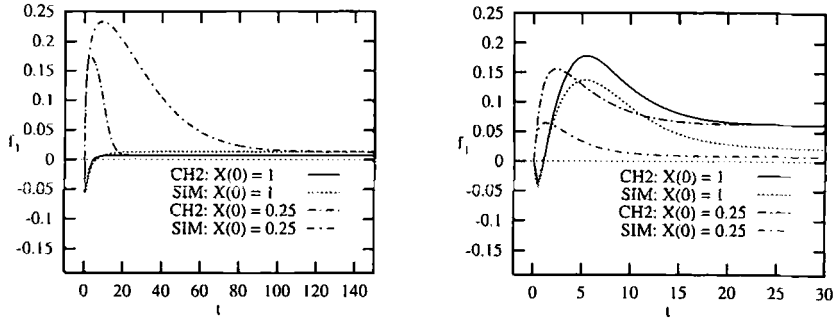

Fig. 10. Evolution of fluctuation correlation $f_1(t)$ for two-species trimolecular model in $d=2(z=4)$ from simulations (SIM) and CH2 for parameter sets 1′ (left) and 2′ (right).

the distribution of transient values of $f_1(t)$ obtained from simulations in Figs. 9 and 10, as we shall do later in this section.

Thus we now write the evolution equation (18) in the form

$$\frac{dX}{dt} = f(X) + \xi_0(t) + g(X)\,\xi_1(t) \tag{21}$$

where $f(X) = -\partial V/\partial X$ and the multiplicative noise function is $g(X) = -(k_1 + k_1')\,X/2$. The potential

$$V(X) = V_0(X) + \tfrac{1}{4}(k_1 + k_1')\,X^2 f_1(\infty) \tag{22}$$

with $V_0(X)$ given by Eq. (4) now contains the constant part of the total effective potential. An additive Gaussian white noise $\xi_0(t)$ obeying Eq. (20) has been included in Eq. (21) to avoid singularities at the zeros of the multiplicative noise function $g(X)$, in this case at $X=0$. Since additive noise does not change the positions of the minima of the potential, this inclusion does not affect our results. Adopting the Stratonovich stochastic differential equation convention[12] (for white noise as the limit of a more general and realistic noise), we find that the evolution of the probability distribution corresponding to Eq. (21) is given by the following Fokker–Planck equation:

$$\frac{\partial P(X,t)}{\partial t} = -\frac{\partial}{\partial X}[K(X)\,P(X,t)] + \frac{\varepsilon_0}{2}\frac{\partial^2}{\partial X^2}P(X,t) + \frac{\varepsilon_1}{2}\frac{\partial^2}{\partial X^2}[g^2(X)\,P(X,t)] \tag{23}$$

where $K(X) = f(X) + \frac{1}{2}\varepsilon_1 g(X)\, g'(X)$. The steady-state solution of Eq. (23) is then

$$P^0(X, t) = \exp\left[2 \int^X \frac{f(z) - (\varepsilon_1/2)\, g(z)\, g'(z)}{\varepsilon_0 + \varepsilon_1 g^2(z)}\, dz \right] = \exp\left[-\frac{V_{\text{eff}}(X)}{\varepsilon_0} \right] \tag{24}$$

where the effective potential for the Fokker–Planck equation with multiplicative noise is given by[13]

$$V_{\text{eff}}(X) = 2 \int^X \frac{\varepsilon_0 (f(z) - (\varepsilon_1/2)\, g(z)\, g'(z))}{\varepsilon_0 + \varepsilon_1 g^2(z)}\, dz \tag{25}$$

For $f(z)$ and $g(z)$, taking the forms given above in (21) and (22), we obtain

$$\begin{aligned} V_{\text{eff}}(X) = & \left[\frac{k_1 + k_1'}{2\beta^2} - \frac{k_2 + k_2'}{2\beta} - \frac{(k_1 + k_1')\, f_1(\infty)}{4\beta} - \frac{\varepsilon_1 (k_1 + k_1')^2}{8\beta} \right] \ln(1 + \beta X^2) \\ & - \left(\frac{k_1}{\beta^{3/2}} - \frac{k_2'}{\beta^{1/2}} \right) \tan^{-1}(\beta^{1/2} X) \\ & - \frac{k_1 + k_1'}{2\beta} X^2 + \frac{k_1}{\beta} X - \frac{k_1 + k_1'}{2\beta^2} \end{aligned} \tag{26}$$

where $\beta = \varepsilon_1 (k_1 + k_1')^2 / 4\varepsilon_0$. The form of this effective potential $V_{\text{eff}}(X)$ is plotted in Fig. 11 on the left for parameter set 1′ [with $f_1(t \to \infty) = 0$ from the left graph of Fig. 9], and a transition to a monostable potential with stable state at $X_1 = 0$ is observed between $\sigma \simeq 0.3$ and $\sigma \simeq 0.4$. This is consistent with the widths of the distribution of transient values of the fluctuation correlation f_1 at $d = 2$ ($\sigma \sim 0.3$) and $d = 1$ ($\sigma \sim 0.4$), from the left graphs of Figs. 10 and 9, and with the transition from the macroscopically more stable steady state at X_3 for $d = 2$ to the macroscopically less stable one at $X_1 = 0$ for $d = 1$ as observed in Figs. 5 and 3, respectively. Likewise for parameter set 2′ the transition to a monostable potential occurs at a critical width $\sigma_c \simeq 0.09$ of the transient fluctuation correlation distribution. In Fig. 11 the potential is plotted for parameter set 2′ on the right for a value $\sigma \sim 0.12$ just above the transition and another $\sigma \sim 0.20$ corresponding to $d = 2$ (see right graph of Fig. 10) to show that the fluctuation correlations are large enough even in $d = 2$ to change the steady state and also make the potential monostable. This is consistent with the results from simulations (Figs. 4 and 6), indicating that the crossover to macroscopic behavior occurs at a dimension greater than two and the corresponding effective potential V_{eff} has a unique stable state for both $d = 1$ and $d = 2$.

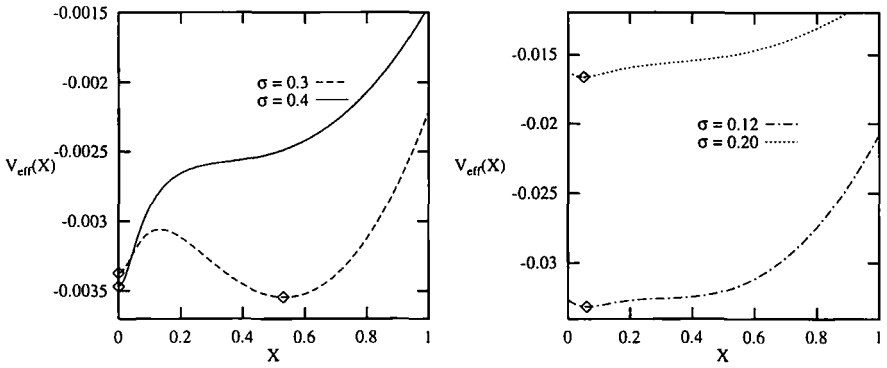

Fig. 11. Effective potential with multiplicative noise: parameter sets 1′ (left) and 2′ (right), $\varepsilon_0 = 0.001$ for two different values of the width σ of the noise distribution corresponding to $d = 1 (z = 2)$ and $d = 2 (z = 4)$ widths for the transient fluctuation correlations. Minima are indicated by diamonds.

Moreover, this stable state corresponds to a concentration X_{eff} that is *not* a stable state of the macroscopic potential and lies somewhat below the macroscopically less stable state $X_1 = 0.1$ (see Fig. 11), again in very good agreement with simulational results shown in Figs. 4 and 6.

We have thus presented an analysis of the modification of the effective potential and the resulting steady states and dynamics of the bistable Schlögl-type models in low spatial dimension. We see that this description of the transient fluctuation correlations as Gaussian white noise gives, in addition to the qualitative analysis of Section 3, a reasonable quantitative agreement with simulations.

5. THE FIRST SCHLÖGL MODEL AND ITS TWO-SPECIES EQUIVALENT

The first Schlögl model, given by the reactions of Eq. (1) with $n = 2$, again with concentrations A and B kept constant by contact with a reservoir, is described by the macroscopic evolution equation

$$\frac{dX}{dt} = -k_1' X^2 + \alpha X - k_2 X + \gamma = -\frac{\partial V_0(X)}{\partial X} \tag{27}$$

where $\alpha = k_1 A$ and $\gamma = k_2' B$. For $\gamma = 0$ the steady state at $X_2 = (\alpha - k_2)/k_1'$ is stable for $k_2 < \alpha$ and unphysical as well as unstable otherwise. $X_1 = 0$ becomes stable for $k_2 \geqslant \alpha$. The transcritical bifurcation diagram for $\gamma = k_2' = 0$ is shown by solid lines in Fig. 12. The other parameter values are $k_1 = 14.0$, $k_1' = 1.0$, $A = 0.05$, and $B = 0.05$.

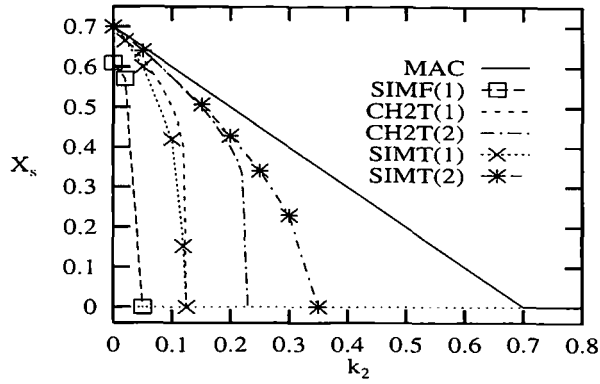

Fig. 12. Steady-state values of concentration for Schlögl's first model vs. reaction rate k_2: from macroscopic theory (MAC), full Schlögl model I in $d=1$ [SIMF(1)], two-species bimolecular model for $d=1$ [SIMT(1)] and $d=2$ [SIMT(2)] from simulations, and from CH2 in $d=1$ and $d=2$. Solid line indicates the stable state and dotted line the unstable state for the macroscopic case. The parameters used are $k_1=14.0$, $k_1'=1.0$, $k_2'=0$, $A=0.05$, and $B=0.05$ for the full Schlögl model and the equivalent ones $k_1=0.7$, $k_1'=0.3$ and $k_2'=0$ for the two-species model.

On the other hand, simulations using the same parameters show that in $d=1$ the state $X_1=0$ becomes stable already at a value of $k_2\simeq 0.04$ far below $\alpha=0.7$ (see again Fig. 12).

In the above simulations the concentrations A and B are maintained constant in the same way as was done for model II discussed in Section 3.

Now we shall proceed to analyze this behavior in terms of the corresponding two-species model as we did in the preceding sections for Schlögl's second model. In analogy with (3), this consists of the reaction steps

$$\begin{aligned} \mathrm{A}+\mathrm{X} &\underset{k_1'}{\overset{k_1}{\rightleftharpoons}} 2\mathrm{X} \\ \mathrm{X} &\underset{k_2'}{\overset{k_2}{\rightleftharpoons}} \mathrm{A} \end{aligned} \tag{28}$$

once again consisting of only A and X particles on a fully occupied lattice, $A=1-X$. The macroscopic evolution equations are

$$\frac{dX}{dt}=-(k_1+k_1')\,X^2+(k_1-k_2-k_2')\,X+k_2'=-\frac{\partial V_0(X)}{\partial X} \tag{29}$$

Thus, for macroscopic behavior to be equivalent to the full model (27) it suffices to substitute parameters $k_1'\to k_1+k_1'$, $\alpha\to k_1-k_2'$, and $\gamma\to k_2'$.

This model with equivalent parameters (see Fig. 12) also shows a transition to a stable state of $X_1 = 0$ at a value of $k_2 \simeq 0.12$ for $d = 1 (z = 2)$ and $k_2 \simeq 0.31$ for $d = 2 (z = 4)$, both significantly below the macroscopic one of $k_2 = 0.7$.

We now solve the master equation (5) for this model using the methodology of Section 3. The transition probability w_j for the first reaction in (28) on a lattice of coordination number z can again be written in the form (12), where now w_j^0 is given by

$$w_j^0(\sigma_j \to -\sigma_j) = \frac{1}{2z} \sum_{c_j} \frac{1 - \sigma_{c_j}}{2} \tag{30}$$

and constructed to obey the conditions that it should be proportional to the probability of finding at least one X particle among the z neighbors of the particle at j and should also be proportional to k_1 if the site j contains an A particle and to k_1' if it contains an X particle. Substituting (30) in the expression (6) while once again assuming spatial isotropy, we obtain in analogy with (14)

$$\left(\frac{dq}{dt}\right)_1 = -\frac{1}{2}(k_1 - k_1') - k_1' q + \frac{1}{2}(k_1 + k_1') q^2 + \frac{1}{2}(k_1 + k_1')(f_1 + f_2) \tag{31}$$

The second (unimolecular) reaction $X \rightleftharpoons A$ contributes the same as before as given in Eq. (15). Once again we shall deal only with the pair of coupled equations for the average concentration difference $q(t)$ and the average nn fluctuation correlation $f_1(t)$; these are [from Eqs. (31) and (15)]

$$\frac{dq}{dt} = -\frac{1}{2}(k_1 - k_1' - 2k_2 + 2k_2') - (k_1' + k_2 + k_2') q + \frac{1}{2}(k_1 + k_1') q^2 + \frac{1}{2}(k_1 + k_1') f_1 \tag{32}$$

and [substituting Eq. (31) in Eqs. (7) and (9)]

$$\frac{df_1}{dt} = \frac{1}{z}(k_1 - k_1') + \frac{1}{z}(k_1 + k_1') q + \frac{1}{z} q^2 - \frac{1}{z}(k_1 + k_1') q^3 - (k_1 + k_1') f_1 + \left(1 - \frac{2}{z}\right) q f_1 \tag{33}$$

The solution of this coupled system for $d=1(z=2)$ yields the same results as simulations for the value of $k_2 \simeq 0.12$ at which the crossover of stable states occurs (see Fig. 12) to $X_1=0$. For $d=2(z=4)$ the transition occurs at a somewhat lower value of $k_2 \simeq 0.23$ according to the solution of the coupled system of equations (32) and (33).

We can once again write the evolution equation (32) in the simplified form of Eq. (18) as follows:

$$\frac{dX}{dt} = -\frac{\partial V_0(X)}{\partial X} - \frac{1}{4}(k_1 + k_1')\, f_1 \tag{34}$$

Inserting the steady-state value of f_1 (see Fig. 13) into the effective potential $V_{\text{eff}}(X) = V_0(X) + V_{\text{fl}}(X)$ of this dynamics as was done at the end of Section 3 for the trimolecular model, we identify the contribution from fluctuations to be of the form [from Eq. (34)] $V_{\text{fl}}(X) = \frac{1}{4}(k_1 + k_1')\, Xf_1$. The form of the resulting effective potential for a time-independent f_1 corresponding to the asymptotic value $f_1(t \to \infty)$ for the $d=1(z=2)$ case shown in Fig. 13 is depicted on the right of Fig. 14. Results of simulations as well as CH2 displayed on the left of Fig. 14 indicate that the stable state is shifted to lower concentrations as compared to the macroscopic one, in agreement with the corresponding effective potential plotted on the right of the same figure. Since the noise term that would be obtained by substituting Eq. (19) in Eq. (34) is purely additive, it does not change further the position of the minima of the potential and is thus irrelevant for the purpose

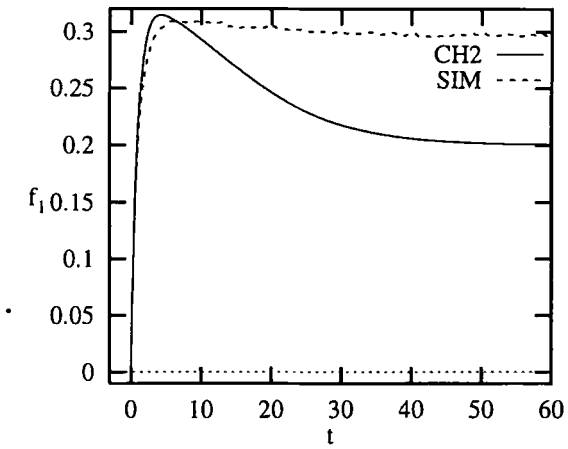

Fig. 13. Evolution of fluctuation correlations $f_1(t)$ for $d=1$ for the same rates as in Fig. 12 with $k_2=0.1$.

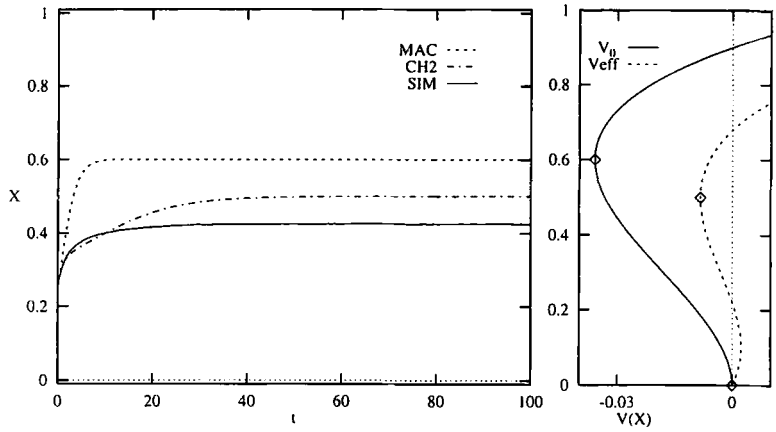

Fig. 14. Evolution of average concentration $X(t)$ for the bimolecular two-species model from macroscopic theory (MAC), solution of CH2, and simulations (SIM) for parameters as in Fig. 13. The right graph shows the corresponding macroscopic potential V_0 and the effective potential V_{eff} with $f_1 = 0.2$ with minima indicated by diamonds.

of this study. Indeed, the substitution of the stationary value of f_1 in Eq. (34) already describes the behavior observed in the simulations. It is to be emphasized, however, that the asymptotic value $f_1(t \to \infty)$ is a function of the parameters and the value of X from the coupled equations (32) and (33). It decreases with k_2 and is zero for $k_2 > \alpha$, where the validity of the macroscopic equation (29) is restored and $X_1 = 0$ is the absorbing state. Moreover, the variation of the term $V_0(X) = \frac{1}{4}(k_1 + k_1')\, Xf_1(t \to \infty)$ with k_2 determines the form of the transition in Fig. 12: as k_2 increases, the macroscopic minimum X_2 comes closer to $X_1 = 0$ and the minimum of V_{eff} at X_{eff} becomes shallower (see right of Fig. 14 with $X_{\text{eff}} = 0.5$). At a critical value of k_2, $X_2 - X_1$ becomes small enough for the additive fluctuation term V_0 to be enough to make the minimum at X_{eff} disappear altogether in favor of one at $X_1 = 0$, thus leading to the sharp transition shown in Fig. 12. This is in contrast to the macroscopic case, where the minimum shifts continuously toward $X = 0$.

Thus we find that the nature of the transition at $k_2' = 0$ between nonzero and zero stable-state concentrations marked by the transcritical bifurcation for the macroscopic version of Schlögl's first (bimolecular) model is somewhat different on a low-dimensional lattice. The bifurcation subsists, but the linear relation $X_2 = (\alpha - k_2)/k_1'$ for the steady-state value of the concentration is replaced by a curve of the form shown in Fig. 12 with a sharp transition to a stable state of $X = 0$ at a critical value of k_2 that is considerably lower than the macroscopic one, $k_2 = \alpha$. This critical value

increases in going from $d=1$ to $d=2$, however, and we expect the curves to approach continuously the macroscopic line as d is increased. We have modeled this behavior by an effective potential that contains an additional term linear in X and proportional to the nn fluctuation correlation f_1.

6. CONCLUSION

We have analyzed the anomalous behavior of some prototype nonequilibrium models of the Schlögl type when embedded in lattices of low spatial dimension. Starting from a Glauber-type master equation supplemented by a truncation procedure, we have obtained evolution equations that incorporate the role of fluctuation correlations. These equations also led us to introduce an effective potential that determines the steady states and dynamics of the system when the fluctuation correlations are appreciable—typically, when the spatial dimension is low.

We find that the transcritical bifurcation for bimolecular models of the Schlögl type I is modified at low dimension and occurs at significantly lower values of k_2. This transition between a steady state at nonzero concentration X_2 to one at $X_1=0$ is more abrupt as compared to the macroscopic case owing to the interplay between the fluctuation correlations and the macroscopic potential as a function of k_2 in the form of the effective potential. On the other hand, for model II we find that the bifurcation to a bistable regime can disappear altogether, the system being attracted by a unique stable state. More specifically, this unique stable state has been found to be at $X=0$ for the case $k_2'=0$ (where $X_1=0$ is stable also for the macroscopic case, but of much lower stability than the stable state X_3 at higher concentration). For the case $k_2'\neq 0$ the new unique stable state is found to be at a lower concentration than that of the lower stable state X_1 of the macroscopic equations. We note that the transition to this monostable potential depends on the magnitude of the fluctuation correlation f_1 and thus is not important for higher dimensional systems, where f_1 becomes negligible. Already, for the two-species model at $k_2'=0$ we find that there is a crossover at $k_2\simeq 0.02$ from monostable to bistable behavior between $d=1$ and $d=2$ and the stable states for the $d=2$ system are the same as the macroscopic ones for low values of k_2. For the full model this crossover seems to occur at $k_2\simeq 0$. Thus we believe that the critical dimension is $d_c\sim 2$ for the crossover to bistable behavior at $k_2'=0$. Below this dimension the behavior is described by a monostable potential for all values of k_1, k_1', and k_2. However for $k_2'\neq 0$ the potential is monostable for $d=2$ for the entire range of parameter values for the two-species model as well as for the full model and the crossover must occur for $d_c\geqslant 2$. To demonstrate this, we have used parameters sets 1, 1′, 2, 2′ such

that macroscopically the stable state at lower concentration is just barely stable, with the one at higher concentration being highly stable, so that a transition to macroscopic behavior can be discerned as soon as it sets in.

We did not see any evidence in model II of a transcritical bifurcation of the type that occurs in model I and was observed in ref. 4 also for model II at low dimension. In contrast to ref. 4, where a sharp transition from one unique steady state to another is observed when k_2 is varied with $k_2' = 0$ for $d < 4$, we observe only a single steady state for dimensions $d \leqslant 2$, with bistability just appearing at $d = 2$. Moreover, the type of transition observed in ref. 4 would not be consistent with our picture of a modified quartic potential in which the bistable regime disappears in the presence of significant fluctuation correlation to yield a unique stable state at low (for $k_2' \neq 0$) or zero (for $k_2' = 0$) concentration. Presumably, the difference with the results of ref. 4 are due to the different ways of modeling the reactive steps and the different assumptions on the allowed occupations of the lattice sites by A, B, and X particles. In particular, the reactions are implemented in ref. 4 on a single site and thus some of the lattice constraints are not incorporated. On the other hand, ref. 14 does incorporate these constraints, but their interest is in identifying a model that exhibits a first-order transition in one dimension of the type exhibited by model II macroscopically. By contrast, our interest has been to study the change in the behavior of the original Schlögl models on the incorporation of lattice constraints.

The work reported in this paper can be extended in several directions. Of special interest would be to assess the role of dimensionality in systems giving rise to bifurcation of time-periodic solutions or to chaotic dynamics. Furthermore, the role of fluctuations on propagating fronts joining coexisting stable states would be another interesting area to explore in this context.

ACKNOWLEDGMENTS

We would like to thank J. R. Weimar for many useful suggestions and help in preparing figures. S.P. acknowledges a postdoctoral fellowship granted by the Université Libre de Bruxelles. This research is supported in part by the Belgian government under the Poles d'Attraction Interuniversitaires program.

REFERENCES

1. S.-K. Ma, *Modern Theory of Critical Phenomena* (Benjamin, New York, 1976); H. E. Stanley, *Introduction to Phase Transitions and Critical Phenomena* (Oxford University Press, Oxford, 1971).

2. G. H. Weiss and R. J. Rubin, *Adv. Chem. Phys.* **52**:363 (1983); S. Havlin and D. ben-Avraham, *Adv. Phys.* **36**:695 (1987).
3. G. Nicolis and M. Malek Mansour, *J. Stat. Phys.* **22**:495 (1980); M. Malek Mansour, C. van den Broeck, G. Nicolis, and J. W. Turner, *Ann. Phys.* **131**:283 (1981).
4. P. Grassberger, *Z. Phys. B* **47**:365 (1982).
5. A. Tretyakov, A. Provata, and G. Nicolis, *J. Phys. Chem.* **99**:2770 (1995).
6. S. Prakash and G. Nicolis; In preparation.
7. G. Nicolis and I. Prigogine, *Self-Organization in Nonequilibrium Systems* (Wiley, New York, 1977).
8. F. Schlögl, *Z. Physik* **253**:147 (1972).
9. S. Prakash and G. Nicolis, *J. Stat. Phys.* **82**:297 (1996).
10. A. Provata, J. W. Turner, and G. Nicolis, *J. Stat. Phys.* **70**:1195 (1993).
11. R. J. Glauber, *J. Math. Phys.* **4**:294 (1963).
12. H. Malchow and L. Schimansky-Geir, *Noise and Diffusion in Bistable Nonequilibrium Systems* (B. G. Teubner Verlagsgeselleschaft, 1985).
13. W. Horsthemke and R. Lefever, *Noise-Induced Transitions* (Springer-Verlag, Berlin, 1984).
14. R. Dickman and T. Tomé, *Phys. Rev. A* **44**:4833 (1991).